This is a repository copy of *Self-filtering electrical area sensors emerging from deep learning*.

White Rose Research Online URL for this paper:
https://eprints.whiterose.ac.uk/157015/

Version: Accepted Version

Article:
Smyl, D.J. orcid.org/0000-0002-6730-5277 and Liu, D. (2020) Self-filtering electrical area sensors emerging from deep learning. Measurement Science and Technology, 31 (6). 065107. ISSN 0957-0233

https://doi.org/10.1088/1361-6501/ab7314

Reuse
This article is distributed under the terms of the Creative Commons Attribution-NonCommercial-NoDerivs (CC BY-NC-ND) licence. This licence only allows you to download this work and share it with others as long as you credit the authors, but you can't change the article in any way or use it commercially. More information and the full terms of the licence here: https://creativecommons.org/licenses/

Takedown
If you consider content in White Rose Research Online to be in breach of UK law, please notify us by emailing eprints@whiterose.ac.uk including the URL of the record and the reason for the withdrawal request.

eprints@whiterose.ac.uk
https://eprints.whiterose.ac.uk/

Measurement Science and Technology

ACCEPTED MANUSCRIPT

Self-filtering electrical area sensors emerging from deep learning

To cite this article before publication: Danny J Smyl *et al* 2020 *Meas. Sci. Technol.* in press https://doi.org/10.1088/1361-6501/ab7314

Manuscript version: Accepted Manuscript

Accepted Manuscript is "the version of the article accepted for publication including all changes made as a result of the peer review process, and which may also include the addition to the article by IOP Publishing of a header, an article ID, a cover sheet and/or an 'Accepted Manuscript' watermark, but excluding any other editing, typesetting or other changes made by IOP Publishing and/or its licensors"

This Accepted Manuscript is **© 2020 IOP Publishing Ltd**.

During the embargo period (the 12 month period from the publication of the Version of Record of this article), the Accepted Manuscript is fully protected by copyright and cannot be reused or reposted elsewhere.
As the Version of Record of this article is going to be / has been published on a subscription basis, this Accepted Manuscript is available for reuse under a CC BY-NC-ND 3.0 licence after the 12 month embargo period.

After the embargo period, everyone is permitted to use copy and redistribute this article for non-commercial purposes only, provided that they adhere to all the terms of the licence https://creativecommons.org/licences/by-nc-nd/3.0

Although reasonable endeavours have been taken to obtain all necessary permissions from third parties to include their copyrighted content within this article, their full citation and copyright line may not be present in this Accepted Manuscript version. Before using any content from this article, please refer to the Version of Record on IOPscience once published for full citation and copyright details, as permissions will likely be required. All third party content is fully copyright protected, unless specifically stated otherwise in the figure caption in the Version of Record.

View the article online for updates and enhancements.

This content was downloaded from IP address 143.167.30.166 on 13/02/2020 at 16:29

Self-filtering electrical area sensors emerging from deep learning

Danny Smyl[1,2]

[1]Department of Civil and Structural Engineering, The University of Sheffield, Sheffield, UK
[2]The Integrated Civil and Infrastructure Research Centre (ICAIR), Sheffield, UK

E-mail: d.smyl@sheffield.ac.uk

Dong Liu[2,3,4]

[3]Hefei National Laboratory for Physical Sciences at the Microscale and Department of Modern Physics, University of Science and Technology of China, Hefei 230026, China
[4]CAS Key Laboratory of Microscale Magnetic Resonance, University of Science and Technology of China, Hefei 230026, China
[5]Synergetic Innovation Center of Quantum Information and Quantum Physics, University of Science and Technology of China, Hefei 230026, China

E-mail: dong2016@ustc.edu.cn

Abstract. In this work, we introduce the concept of self-filtering electrically-conductive area sensors for use in nondestructive evaluation, state estimation, and other contemporary engineering applications. For this, a deep learning-based approach is used to optimize sensors' conductivity distributions in order to minimize the effect of noise on Electrical Impedance Tomography (EIT) reconstructions. From sensor design examples, it is shown that (a) the underlying physical self-filtering mechanism arising from the deep learning-based approach functions by reducing the sensitivity of the internal electric potential field to noise perturbations and (b) the use of optimized self-filtering sensors can improve the robustness to noise by approximately 25% compared to standard homogeneous sensors. Lastly, using an alternative interpretation of the self-sensing optimization problem, it is shown that fundamental connections between modeling errors, measurement noise, and physics of self-filtering sensors can be linked and unlocked using deep learning.

Keywords: Electrical Impedance Tomography, inverse problems, nondestructive evaluation, structural health monitoring, tomography

1. Introduction

The use of self-sensing materials and electrically-conductive engineered sensors has recently been the source of significant research in the areas of nondestructive testing [1, 2, 3, 4], mechanical property characterization [5, 6, 7, 8], state estimation [9, 10, 11], and more. Yet, despite the growing prevalence of electrical modalities (e.g. Electrical Impedance Tomography (EIT), Electrical Capacitance Tomography, and inductance-based modalities) and the practical need for improving electrical sensor quality, information regarding the optimization electrical sensors themselves is scarce. In the case of EIT – the central focus application in this work – there are a few exceptions, namely works focused on electrode position optimization [12, 13, 14, 15]. However, to the authors' knowledge, the optimization of the conductive sensing area itself has yet to be explored.

In this work, we address this realization by introducing the conceptual basis and design of "self-filtering" electrically conductive area sensors. By "self-filtering" we refer to a passive system whereby the electric properties (in this case the conductivity distribution) act as a filter to increase the robustness of the area sensor to random noise. Put differently, and in the context of EIT as it pertains to this work, a "self-filtering" area sensor is one that minimizes the the effects of random noise on EIT reconstructions. Of course, the concept of noise reduction in electrical systems is not unprecedented; for example, the use of capacitors in

Accepted Manuscript

electric circuits is wildly adopted to reduce/cancel/decouple systematic and/or random noise in electrical signals [16]. Nonetheless, the optimization of two-dimensional electric properties for improving EIT sensor properties remains to be explored.

We undertake the self-filtering sensor design problem using a deep learning-based approach to determine optimal conductivity distributions aiming to minimize the effects of noise on EIT reconstructions. The approach is intended to be straightforward and provide smooth distributions capable of production using contemporary printing technology. We begin by discussing the theoretical self-filtering rationale from an EIT perspective, the deep learning-based optimization approach, and lastly provide some optimized EIT sensor examples, discussion, and conclusions.

2. Self-filtering sensors in the context of EIT

EIT is an inverse problem where we aim to estimate a conductivity distribution σ from boundary voltage measurements V. A central challenge in EIT is the ill-posed nature of the problem, namely that small changes in V result in large changes in σ [17]. In practical applications, these small changes are manifested in unavoidable random noise ϵ. In the context of engineering applications where we have the ability to manufacture EIT sensors, it is logical to ask: *can we design a conductivity distribution σ to minimize the effects of ϵ on EIT reconstructions*?

Such a conductivity distribution would therefore serve as a simple filter with respect to randomized noise. As a consequence, the optimized distribution σ_{opt} would result in an improvement of EIT's robustness across a given noise spectrum. We can formalize these statement (in the least-squares sense) by writing the theoretical solution for the optimal self-filtering distribution

$$\sigma_{\text{opt}} = \underset{\sigma}{\text{argmin}} \sum_{j=1}^{\infty} ||V_j^{\epsilon} - U(\sigma)||^2 \tag{1}$$

where V_j^{ϵ} are noisy measurements with a standard deviation Σ and U is an accurate EIT model mapping $\sigma \to V$ (in this work we use the finite element version of the complete electrode model [18]). In theory, we would then obtain σ_{opt} when $\sum_{j=1}^{\infty} ||V_j^{\epsilon} - U(\sigma_{\text{opt}})||^2 = 0$. Of course, we cannot take an infinite number of samples in practice, so we substitute a finite number of sample N by writing

$$\sigma_{\text{opt}} \approx \underset{\sigma}{\text{argmin}} \sum_{j=1}^{N} ||V_j^{\epsilon} - U(\sigma)||^2. \tag{2}$$

Finding an optimal distribution using Eq. 2 is quite daunting on first glance, especially (i) for a large N and (ii) if were were to treat the problem using standard optimization approaches. However, we may circumvent this using deep learning, i.e. treating Eq. 2 as a highly-nonlinear fitting problem as detailed in the following section. In doing this using any approach however, it must be noted that estimates for σ_{opt} are only valid for the range of Σ (and other errors) considered.

3. Deep learning-based sensor optimization

In this section we aim to derive the optimal self-filtering conductivity distribution σ_{opt} using a trained neural network $\mathcal{A}$. To do this, we first aim to learn the nonlinear mapping

$$\sigma = \mathcal{A}(||V - U(\sigma)||^2) \tag{3}$$

using N sets of training data comprised of noise-corrupted data V^{ϵ} and randomized conductivity distributions σ_t. We immediately notice, however, that the optimal conductivity distribution is obtained when $||V - U(\sigma)||^2 = 0$; thus, the optimized self-filtering sensor is computed using

$$\sigma_{\text{opt}} = \mathcal{A}(0). \tag{4}$$

In this work, we do not assume that the network $\mathcal{A}$ is generalized for a large suite of different EIT geometries, meshes, electrode configurations, measurement patterns, and current injection patterns. Rather,

Accepted Manuscript

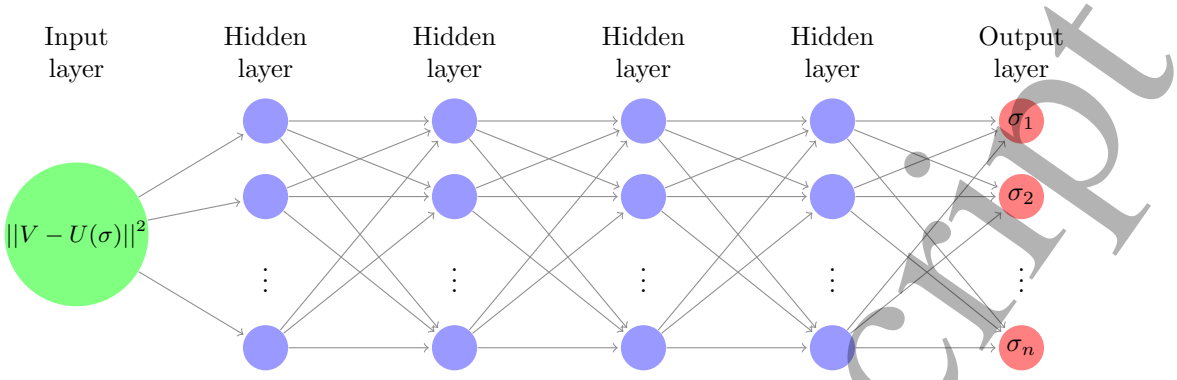

Figure 1. Schematic illustration of the trained model for the nonlinear mapping $\sigma = \mathcal{A}(||V - U(\sigma)||^2)$. A discretization of σ is shown on the right hand side of the diagram consisting of n nodal values for σ.

we assume that $\mathcal{A}$ is only valid when each one of the former features is uniquely defined (i.e., one mesh, electrode configuration, injection/measurement pattern, etc.).

In selecting the network, we choose a feedforward network (shown schematically in Fig. 1) with four hidden layers, where 100 neurons per hidden layer with ReLU activation functions are chosen based on trial and error. We note that the use of additional layers and neurons is found to result in instability of the predicted conductivity distributions, which is likely the result of overfitting. To train the network, Keras/TensorFlow [19] is utilized on a Spyder/Python platform with random dropout rate of 0.2 per layer to improve the network's robustness. This network selection ensures the computations can be pragmatically tractable on the available resources (8-core Xeon processor and 32 Gb RAM) using the stopping criterion defined by the MSE of the network predictions as follows: MSE $\leq 10^{-4}$.

It should be noted that the regularization parameter $\lambda = 0.1$ was fixed throughout this work for simplicity. In the network, we employ an L_2 regularization scheme such that the objective function is weighted as follows

$$\Phi = \frac{1}{N}\sum_{i=1}^{N}(\sigma_i^d - \sigma_i^Q)^2 + \lambda R \tag{5}$$

where $R = ||w||^2$, w are the network weights, σ_i^d is the desired output and σ_i^Q is the output from the network at sample i. As seen n Eq. 5, the selection of λ has an effect on the degree of data fitting and therefore biases σ_{opt}. In future work, this issue will be addressed using Bayesian adaptive regularized networks.

4. Examples: optimized self-sensing EIT area sensors.

In this section, we provide illustrating examples of optimized self-filtering conductivity distributions using different geometries. In each example, we consider $N = 10,000$ noise-corrupted voltage data sets V^ϵ corresponding to 1000 randomized conductivity distributions within the range $1 \leq \sigma_t \leq 10$ mS/cm (a common range for painted EIT sensing skins). To obtain the randomized conductivity samples, an isotropic Gaussian smoothness prior was used as a seed to generate blob-like samples using a correlation length equal to half of the diameter or short side length (if the geometry was a circle or rectangle, respectively). In generating the noisy data, Gaussian noise with a standard deviation in the range $0.1\% \leq \Sigma \leq 10\%$ was added to simulated voltages computed using complete electrode model. In addition to this, random noise (with the same standard deviation) was added to homogeneous contact impedances set to $z = 10^{-5}$. All data was sampled using standard adjacent electrode potential measurements and 1mA opposite current injections. Lastly, during training, 10% of the data was used for validation and an independent data set (50% the size of the training data) was used for verification.

We would like to remark that since the training data used herein is generated using finite element simulations, the usefulness of the learned mapping is dependent on the accuracy of the finite element solutions. Indeed, the density of the finite element mesh, especially near the electrodes, has a significant effect on the accuracy of solutions to the EIT forward problem [20]. In particular, EIT forward solutions may be unreliable when (a) the number of elements in contact with the electrodes is low and (b) when the mesh density is very

Accepted Manuscript

coarse. In these cases, the finite element solutions may be highly inaccurate and the simulated voltages may contain significant modeling errors. Above a certain threshold, modeling errors dominate, the training data becomes unreliable, and the resulting learned mapping yields meaningless predictions. To ensure the meshes are sufficiently accurate in this work, we select mesh densities that were experimentally validated in [3, 2].

4.1. Circular geometry

In this first example, we examine a circular geometry with a radius $R = 10$ cm and $E = 6$ boundary electrodes. For the FE mesh, we use a triangular discretization with 1082 elements. Based on the optimization approach outlined in section 3, the optimized conductivity distribution shown in Fig. 2a is obtained. We observe that the optimized self-filtering conductivity distribution is radially symmetric, decreasing towards the center, and has a more narrow conductivity range that the sampled random conductivity distributions (approximately $2.5 \leq \sigma \leq 7$ mS/cm compared to $1 \leq \sigma_t \leq 10$ mS/cm, respectively). It is not immediately obvious what effect the optimized conductivity distribution has on the internal electric potential – which is key in understanding the how the optimized distribution improves the robustness to noise.

To investigate this, we consider a current injection between electrodes 1 and 4 and examine the corresponding internal potential distribution in the optimized self-filtering sensor (Fig. 2b, electrode 1 is top right and electrode 4 is bottom left). Since the self-filtering sensor is radially-symmetric, potential distributions corresponding to other opposite current injections yield equivalent results. As a reference, we compare to the same current injection into a sensor with a homogeneous conductivity distribution equal to the mean value of the optimized sensor (Fig. 2c). We notice that the maximum electric potential in the self-filtering sensor is approximately half the magnitude of the homogeneous sensor's maximum potential. Moreover, the spatial gradient of the self filtering sensor's internal electric potential is significantly flatter than than that of the homogeneous distribution. These observations lead us to deduce that the self-filtering conductivity distribution has an averaging effect on the internal potential distribution.

Based on the former realizations, we conclude that the physical "self-filtering mechanism" of the optimized sensor's conductivity distribution works by decreasing the sensitivity of the internal electric potential field (and therefore the boundary electrode potentials) to perturbations in the in the injected currents. Conversely, via Ohm's law, this is equivalent to stating that the self-filtering conductivity distribution decreases the sensitivity of potential measurements to perturbations in the internal current density distribution. Given the latter, it is therefore expected that the increase in self-filtering EIT sensor robustness to measurement noise comes at the loss of reconstruction accuracy. This would be due to a reduction in sensitivity of the measurements to changes in conductivity (and local current density). Such a change would be particularly important to consider in sensor design when changes are expected far from the domain boundaries, where EIT is least sensitive. Therefore, and to sum up this subsection, a pragmatically optimal EIT sensor is likely not one with only "maximal" self-filtering properties; but, rather, one that where self-filtering properties and sensitivity to distant conductivity changes are considered simultaneously. Addressing this issue will be reserved for future work.

Accepted Manuscript

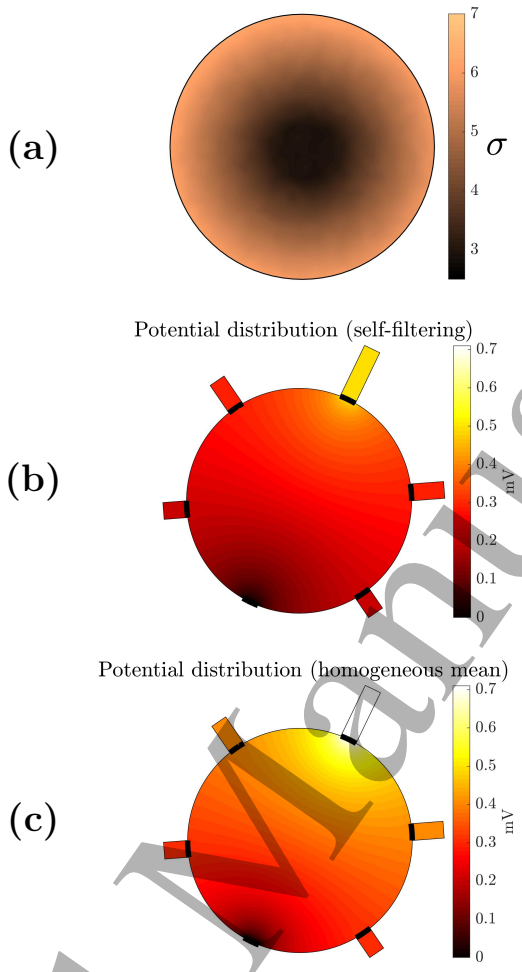

Figure 2. Distributions plotted atop the example circular geometry corresponding to (a) the optimized self-filtering conductivity, (b) electric potential field for a single current injection into the self-filtering sensor, and (c) electric potential field for a single current injection into a homogeneous conductivity distribution (the mean value of the self-filtering conductivity distribution). Relative electrode potentials are illustrated as rectangles protruding from the electrodes.

4.2. Square and rectangular geometries

In this subsection we demonstrate optimized self-filtering conductivity distributions for a 10×10 cm square geometry and a 10×20 cm rectangular geometry. The square and rectangular geometries considered have $E = 8$ and 10 electrodes with 484 and 662 elements in the FE mesh, respectively (see Fig. 3(a,b)). The optimized conductivity distributions computed using the approach in section 3 are shown in Fig. 3(c,d). Upon immediate inspection of the optimized distributions, we observe an "X-shaped" conductivity distribution, where the conductivity is highest near the center of the electrode locations and decreases towards the diagonals connecting the corners. This is in contrast to the symmetric distributions observed in the circular example and results from the asymmetry of the electrodes and geometries. We also observe that the optimized distributions are not completely symmetric about the lines connecting the midpoints of opposite sides, which is an artifact resulting from errors or biases (selection of λ) in the learned model.

As with the previous example, it was found that the self-filtering sensors also had the effect of decreasing the sensitivity of the internal electric potential field to perturbations in the injected current. For the sake of brevity, and due to the fact that the internal potential field is not the same for every opposite current excitation pattern do to asymmetry, we do not show potential distribution comparisons in the example. Rather, we quantify the sensitivity of the internal potential field using the standard deviation (Σ_V) of the

Accepted Manuscript

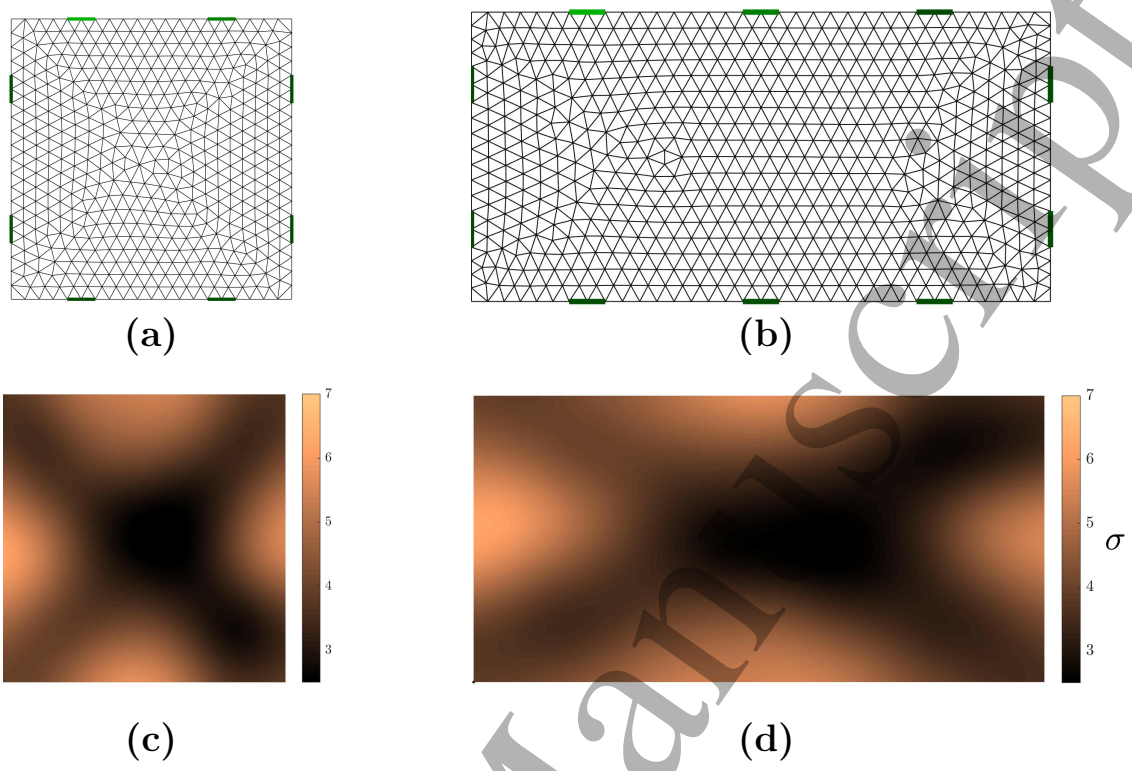

Figure 3. Square and rectangular geometry FE meshes (top row) and optimized self-filtering conductivity distributions (bottom row).

internal potential gradient magnitudes $\bar{V}_k = \sqrt{(\nabla_x V_k)^2 + (\nabla_y V_k)^2}$ – considering all current injections – as a metric by writing

$$\Sigma_V = \sqrt{\frac{\sum_{k=1}^{K} (\bar{V}_k - \mu_{\bar{V}})^2}{K-1}} \tag{6}$$

where $\mu_{\bar{V}}$ is the mean of $\bar{V}$ with g nodes, ι current injections, and a total of $K = g \times \iota$ sample points. Using this metric, conductivity distributions with a lower Σ_V value correspond to internal potential fields (and also electrode potentials) that are less sensitive to changes/perturbations in the injected currents than conductivity distributions with higher Σ_V values. Using the Ohm's Law interpretation described earlier, a lower Σ_V value would also correspond to lower electrode sensitivity to perturbations in the internal current density field. In other words, Σ_V may be interpreted as a term which measures the sensitivity or robustness of electrode measurements to internal changes in the electric current. As it pertains to this work, lower Σ_V values correspond to increased "self-filtering" properties and EIT reconstructions' robustness to noise (i.e changes in ϵ have less affect on reconstructions).

We begin our quantitative investigation by comparing Σ_V values from the optimized sensors to Σ_V values from sensors with homogeneous conductivities equal to the mean of the self-filtering sensors shown in Fig. 3(c-d). Starting with the square geometry, we obtain $\Sigma_V = 0.210$ and $\Sigma_V = 0.246$ for the self-filtering and heterogeneous distributions, respectively. For the rectangular geometry, we obtain $\Sigma_V = 0.133$ and $\Sigma_V = 0.161$ for the self-filtering and heterogeneous distributions, respectively. These values correspond to an improvement of approximately 25% in measurement robustness by employing the self-filtering sensors, as indicated by indicated by Σ_V. Consistent with the discussion from the previous section, we expect that these improvements in robustness come with a loss in reconstruction accuracy far from the electrodes. In future works, we aim to address this issue by developing a sensor design regime capable of balancing measurement robustness (Σ_V) and reconstruction accuracy.

Accepted Manuscript

4.3. An alternative explanation for the "self-filtering" mechanism

Until this point, the mechanisms underlying self filtering have been discussed in physical terms. However, if we re-examine Eq. 2, we notice that the equation can be reinterpreted if we first observe that the noisy simulated data can be rewritten as

$$V^{\epsilon} = R_1(\sigma)I + \varepsilon \tag{7}$$

and

$$U(\sigma) = R_2(\sigma)I \tag{8}$$

where R_1 and R_2 are the FEM matrices, I is a fixed vector of injected currents, and ε is an additive noise vector. Now by substituting the matrix terms into Eq. 2, we have

$$\sigma_{\text{opt}} \approx \underset{\sigma}{\text{argmin}} \sum_{j=1}^{N} ||R_1(\sigma_j)I + \varepsilon_j - R_2(\sigma)I||^2. \tag{9}$$

where $\sigma_j \in \sigma_t$ is a sample conductivity distribution and ε_j is random noise vector. Moreover, the argument input evaluated at j is at a minimum (0) when

$$R_1(\sigma_j)I + \varepsilon_j - R_2(\sigma)I = 0 \tag{10}$$

or, by rearranging

$$R_1(\sigma_j)I - R_2(\sigma)I = [R_1(\sigma_j) - R_2(\sigma)]I = -\varepsilon_j \tag{11}$$

assuming R_1 and R_2 are the same size. The interpretation from Eq. 11 is that the optimization regime is essentially matching the accuracy of the numerical models (or their differences) to the errors of in the data ε. Therefore, recalling that the global optimum is achieved herein by substitution into the learned model, i.e. $\sigma_{\text{opt}} = \mathcal{A}(0)$, we conclude that the deep learning regime predicts the the solution

$$\mathcal{A}(0) \approx \sigma_{\text{opt}} \approx \underset{\sigma}{\text{argmin}} \sum_{j=1}^{N} ||R_1(\sigma_j)I - R_2(\sigma)I + \varepsilon_j||^2. \tag{12}$$

This is a very intuitively-interesting result for several reasons, but one in particular. In the process of developing a learned model linking the accuracy of numerical models and data to conductivity, the model has simultaneously unlocked physical connections underlying the mechanisms behind the self-filtering process in EIT sensors (detailed in the previous subsections). While the importance of linking numerical model accuracy to data quality has recently been established [21, 22] for inverse problems: we feel that deep learning may open the door to uncovering more profound/fundamental understandings behind the physics of sensors used as targets for non-linear and ill-posed imaging approaches. Moreover, due to the high-dimensionality (and ill-posedness/non-linearity) of this and related sensor optimization problems, the use of traditional inverse methods for uncovering such physics would likely be quite challenging.

5. Concluding remarks

In this work, we introduced the concept of self-filtering electrical area sensors in the context of Electrical Impedance Tomography (EIT). The "self-filtering" aspect was defined as a conductivity distribution which increases the robustness of EIT reconstructions to measurement noise. In order to obtain the self-filtering distributions, a deep learning-based optimization approach was used. It was found that the underlying physical self-filtering mechanism works by decreasing the sensitivity of the internal electric potential field (and therefore the electrode potentials) to perturbations in the in the injected currents. This realization was quantified using a derived statistical robustness metric and qualified via observing the sensitivity of the internal electric potential distribution to the injected current. Based on this analysis, it was found that the self-sensing distributions can increase measurement robustness by approximately 25%, but this is likely at the loss of reconstruction accuracy far from the electrodes.

Accepted Manuscript

Lastly, an alternative interpretation of the self-filtering optimization approach was identified. In the process – developing a learned model linking the accuracy of numerical models and data to conductivity – it was found that the deep learned model simultaneously unlocked physical connections underlying the mechanisms behind the self-filtering process in EIT sensors. We are therefore encouraged by the potential use of deep learning for use in (a) optimizing area sensors and (b) unlocking new fundamental information on the physics of sensors whose characteristics may have previously been shrouded by non-linearity and/or ill-posedness of the underlying numerical problems.

Acknowledgments

DS would like to acknowledge the support of the Civil and Structural Engineering Department at the University of Sheffield. DS would also like to thank Professor Mohammad Pour-Ghaz (NC State) for many inspiring conversations on related topics over the years. DL was supported by the National Natural Science Foundation of China under Grant No. 61871356.

References

[1] Thomas A, Kim J, Tallman T and Bakis C 2019 *Composites Part B: Engineering* **177** 107276
[2] Hallaji M, Seppänen A and Pour-Ghaz M 2014 *Smart Materials and Structures* **23** 085001
[3] Smyl D, Pour-Ghaz M and Seppänen A 2018 *NDT & E International* **99** 123–133
[4] Kang I, Schulz M J, Kim J H, Shanov V and Shi D 2006 *Smart Materials and Structures* **15** 737
[5] Hassan H and Tallman T N 2019 *Structural Health Monitoring* 1475921719863062
[6] Tallman T N and Wang K 2016 *Structural Health Monitoring* **15** 235–244
[7] Li M, Lin V W, Lynch J P and Li V C 2013 *Special Publication* **292** 1–16
[8] Loh K J, Kim J, Lynch J P, Kam N W S and Kotov N A 2007 *Smart Materials and Structures* **16** 429
[9] Rymarczyk T, Tchórzewski P, Niderla K, Adamkiewicz P and Sikora J 2019 Examination of moisture condition of buildings using electrical tomography *2019 Applications of Electromagnetics in Modern Engineering and Medicine (PTZE)* (IEEE) pp 193–197
[10] Smyl D and Liu D 2019 *IEEE Sensors Letters*
[11] Rashetnia R, Alla O K, Gonzalez-Berrios G, Seppanen A and Pour-Ghaz M 2018 *Materials Evaluation* **76** 1405–1413
[12] Li R, Hao Z, Mu W and Wang X 2019 Optimal design of electrodes for an electrical impedance tomography based flexible sensor *Sensors and Smart Structures Technologies for Civil, Mechanical, and Aerospace Systems 2019* vol 10970 (International Society for Optics and Photonics) p 109702R
[13] Smyl D and Liu D 2019 *arXiv preprint arXiv:1910.10077*
[14] Hyvonen N, Seppänen A and Staboulis S 2014 *SIAM Journal on Applied Mathematics* **74** 1831–1851
[15] Cao Z, Wang H and Xu L 2008 *Review of Scientific Instruments* **79** 103710
[16] Cochrane D, Chen D Y and Boroyevic D 2003 *IEEE Transactions on Power Electronics* **18** 756–763
[17] Mueller J L and Siltanen S 2012 *Linear and nonlinear inverse problems with practical applications* (SIAM)
[18] Vauhkonen P, Vauhkonen M, Savolainen T and Kaipio J 1999 *IEEE T. Biomedical Eng.* **46** 1150–1160
[19] Chollet F 2015 keras `https://github.com/fchollet/keras`
[20] Adler A and Lionheart W R 2011 *Physiological measurement* **32** 823
[21] Smyl D and Liu D 2019 *Journal of Computational Physics* **399** 108949
[22] Burger M, Korolev Y and Rasch J 2019 *Inverse Problems* **35** 024006

Accepted Manuscript